Available online at www.sciencedirect.com

SCIENCE DIRECT®

Journal of Controlled Release 107 (2005) 428–448

journal of controlled release

www.elsevier.com/locate/jconrel

Cationic albumin-conjugated pegylated nanoparticles as novel drug carrier for brain delivery

Wei Lu[a], Yan Zhang[b], Yu-Zhen Tan[c], Kai-Li Hu[a], Xin-Guo Jiang[a,*], Shou-Kuan Fu[b]

[a]*Department of Pharmaceutics, School of Pharmacy, Fudan University (Fenglin Campus), P.O. Box 130, 138 Yi Xue Yuan Rd, Shanghai 200032, People's Republic of China*

[b]*Department of Macromolecular Science of Fudan University and the Key Laboratory of Molecular Engineering of Polymers, Ministry of Education, Shanghai 200433, People's Republic of China*

[c]*Department of Anatomy and Histology and Embryology, Shanghai Medical School, Fudan University, Shanghai 200032, People's Republic of China*

Received 16 August 2004; accepted 25 March 2005

Abstract

In this paper, a novel drug carrier for brain delivery, cationic bovine serum albumin (CBSA) conjugated with poly(ethyleneglycol)–poly(lactide) (PEG–PLA) nanoparticle (CBSA–NP), was developed and its effects were evaluated. The copolymers of methoxy-PEG–PLA and maleimide-PEG–PLA were synthesized by ring opening polymerization of D,L-lactide initiated by methoxy-PEG and maleimide-PEG, respectively, which were applied to prepare pegylated nanoparticles by means of double emulsion and solvent evaporation procedure. Native bovine serum albumin (BSA) was cationized and thiolated, followed by conjugation through the maleimide function located at the distal end of PEG surrounding the nanoparticle's surface. Transmission electron micrograph (TEM) and dynamic light scattering results showed that CBSA–NP had a round and regular shape with a mean diameter around 100 nm. Surface nitrogen was detected by X-ray photoelectron spectroscopy (XPS), and colloidal gold stained around the nanoparticle's surface was visualized in TEM, which proved that CBSA was covalently conjugated onto its surface. To evaluate the effects of brain delivery, BSA conjugated with pegylated nanoparticles (BSA–NP) was used as the control group and 6-coumarin was incorporated into the nanoparticles as the fluorescent probe. The qualitative and quantitative results of CBSA–NP uptake experiment compared with those of BSA–NP showed that rat brain capillary endothelial cells (BCECs) took in much more CBSA–NP than BSA–NP at 37 °C, at different concentrations and time incubations. After a dose of 60 mg/kg CBSA–NP or BSA–NP injection in mice caudal vein, fluorescent microscopy of brain coronal sections showed a higher accumulation of CBSA–NP in the lateral ventricle, third ventricle and periventricular region than that of BSA–NP. There was no difference on BCECs' viability between CBSA-conjugated and -unconjugated pegylated nanoparticles. The significant results in vitro and in vivo showed that CBSA–NP was a promising brain drug delivery carrier with low toxicity.

Keywords: Cationic bovine serum albumin (CBSA); Pegylated nanoparticle; Brain delivery; Blood–brain barrier (BBB); 6-Coumarin

* Corresponding author. Tel.: +86 21 5423 7381; fax: +86 21 5423 7381.
E-mail address: xgjiang@shmu.edu.cn (X.-G. Jiang).

0168-3659/$ - see front matter © 2005 Elsevier B.V. All rights reserved.
doi:10.1016/j.jconrel.2005.03.027

1. Introduction

The blood–brain barrier (BBB) formed by brain capillary endothelial cells and invested by astrocytes foot processes is characterized as its endothelial tight junction and a complete absence of pinocytic activity [1]. The unique property of BBB restricts exogenous substances and drugs to enter the central nervous system (CNS) from systemic circulation. Only small molecules with high lipid solubility and low molecular mass of less than 400–500 Da, actually cross the BBB [2]. The therapeutic efficacies of proteins and gene drugs are discounted because of their hydrophilicities, protein bound properties and large molecular weights.

In order to improve their brain entrance, many non-invasive CNS delivery techniques are adopted. The increase of the lipid solubility of drug facilitates its BBB passive diffusion. Nutrient's mimic drug design or conjugation of drug with nutrient can perform carrier mediated transport via a specific nutrient transport system. Coupling drug with the specific brain transport targetor results in absorptive mediated transcytosis (AMT) or receptor mediated transcytosis (RMT) [3]. However, all of these techniques are complicated for their chemical modifications and limited for their lower drug carrying capacity.

Recently, immunoliposomes, in which the brain specific targetors were covalently conjugated to polyethyleneglycol (PEG) modified liposomes (pegylated liposomes) as drug carrier via the tips of its functional PEG strands, proved to be successful in brain drug delivery. Its advantages over the drug–targetor direct combination technique were the larger drug loading capacity, disguise of limiting characteristics of drugs with physical nature of the liposome and reduction of drug degradation in vivo. The surface modification of PEG enabled the liposomes to escape the arrest of mononuclear phagocytic system (MPS) so as to prolong its half-life in plasma and increase the area under the concentration–time curve (AUC). Huwyler et al. developed mouse monoclonal antibody against the rat transferrin receptor, OX26, coupled with pegylated liposome to delivery drug into CNS through RMT process [4]. This immunoliposome succeeded in the delivery of small molecules such as daunomycin [4] and plasmid DNA [5–8].

In contrast to RMT, AMT may involve endocytosis initiated by the binding of polycationic substances to negative charges on the plasma membrane or by the binding of extracelluar lectins [9]. Cationic bovine serum albumin (CBSA), which was investigated in isolated brain capillaries and evaluated with internal carotid perfusion/capillary depletion technique in vivo, indicated a good accumulation profile in the brain [10]. Both apparent brain homogenate and postvascular supernatant volume of distribution of CBSA were much higher than native bovine serum albumin (BSA) during a 10-min constant rate brain perfusion in rats [11]. CBSA appeared to have favorable pharmacokinetic properties with a longer serum half-life and a greater degree of selectivity to brain tissue as compared to other organs (liver, heart, lung) [3]. Furthermore, compared with the monoclonal antibody, CBSA was easier to prepare. With these traits, CBSA was found to be a promising alternative brain targetor designed to couple with the liposomes. CBSA coupled pegylated liposomes were taken up into brain endothelium via an absorptive mediated endocytotic pathway and proved to be a suitable carrier for brain drug delivery under the confocal laser scanning fluorescence microscopy [12].

Besides liposomes, as the drug container, nanoparticles have certain advantages over liposomes for their function to prolong drug release [13], be freeze-dried for long-term storage and be more chemically and physically stable [14]. They also can be loaded with small molecules, proteins or plasmid DNA with different specific methods [15–18]. Hydrophilic PEG covering the surface area has been found to prolong the blood half-life of poly(lactide) (PLA) nanoparticles in rats up to several hours [19]. The methoxy-polyethyleneglycol–poly(lactide) (MPEG–PLA) nanoparticles seem much less toxic since they were shown to have an acceptable safety profile in rats [20]. This synthetic technical validation of immunonanoparticles was confirmed by Olivier et al. who succeeded in synthesis of OX-26 coupled with pegylated nanoparticles [21].

With these considerations, the purpose of this experiment was to synthesize cationic albumin-conjugated pegylated nanoparticles (CBSA–NP) as a novel drug carrier for brain drug delivery. We used a bifunctional PEG containing a maleimide group at one terminus and free hydroxyl group at the other terminus to initiate maleimide-PEG–PLA. The pegylated nanoparticles were prepared by the blend of this novel copolymer and MPEG–PLA copolymer using emul-

sion/solvent evaporation technique. The molecular weight of PEG in maleimide-PEG was chosen higher than that in MPEG, so that the maleimide function would protrude from the corona to be available for conjugating the thiolated CBSA under the mild condition to form CBSA–NP (Fig. 1). To investigate whether this novel brain drug delivery system was effective or not, a lipophilic fluorescent dye, 6-coumarin, was incorporated into CBSA–NP as a nanoparticle probe. CBSA–NP loaded with 6-coumarin was quantitatively and qualitatively evaluated using an uptake experiment by the rat brain capillary endothelial cells (BCECs) in vitro and visualized its localization in brain tissue sections by fluorescence microscope in vivo, compared with BSA-conjugated pegylated nanoparticles (BSA–NP). The BCECs cytotoxicity of CBSA–NP was also investigated.

2. Materials and methods

2.1. Materials and animals

D,L-Lactide (99.5% pure) was purchased from PURAC and purified by twice recrystallization from dried ethyl acetate. Methoxy-polyethyleneglycol (MPEG, MW 3000 Da) was brought from NOF Corporation (SUNBRIGHT™ MEH-30 H, Lot No. 14530, Japan). Maleimide-polyethyleneglycol (maleimide-PEG, MW 3400 Da) was custom-synthesized (NEKTAR™, Lot No. PT-08D-16, Huntsville, AL). Stannous octate (stannous content: 26.5–27.5%) was supplied by Shanghai Chemical Reagent Company. Bovine serum albumin V (BP0042 Roche) was purchased from Huamei Bioengineering Company (China); 6-coumarin, from Aldrich; dextran

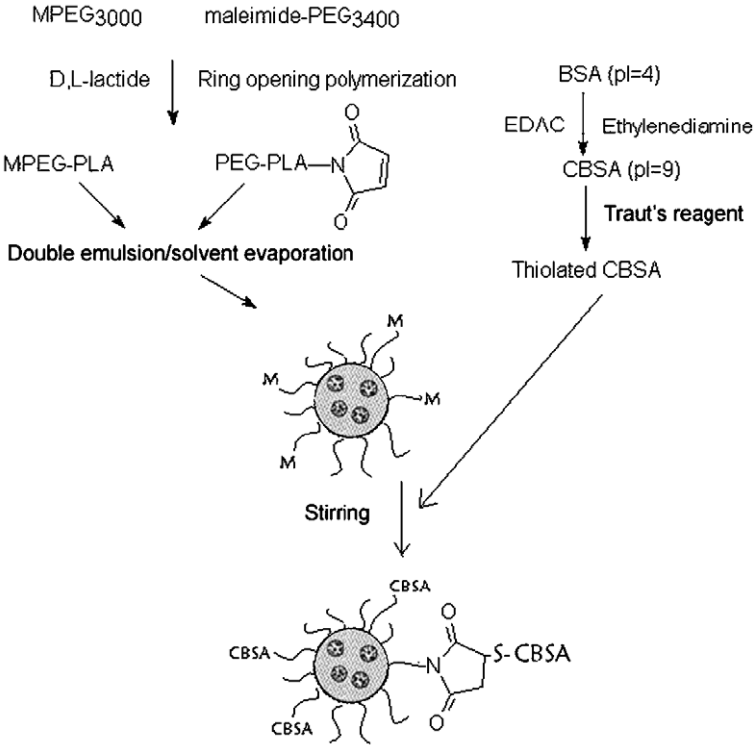

Fig. 1. The schematic diagram of synthesis of CBSA–NP: the copolymers of MPEG–PLA and maleimide-PEG–PLA were synthesized by means of ring opening polymerization, respectively; the pegylated nanoparticles were prepared by the blend of these two copolymers using emulsion/solvent evaporation technique (M represents the maleimide function on the tip of maleimide-PEG–PLA); BSA was firstly cationized with the ethylenediamine in the appearance of 1-ethyl-3-(dimethylaminopropyl)-carbodiimid-hydrochloride (EDAC) and secondly thiolated using Traut's reagent; the thiolated CBSA was conjugated with the pegylated nanoparticles through the mild stirring with reaction of the thiol group and the maleimide group at the room temperature.

(MW ~ 100 kDa), from Fluka Chemie GmbH (Riedel-de Haën Brand, Germany); 1-Ethyl-3-(dimethylaminopropyl)-carbodiimid-hydrochloride (EDAC) and 5,5′-Dithiobis(2-nitrobenzoic acid) (Ellmann's reagent), from Acros (Belgium); heparin™–biotin sodium salt (B9806) and streptavidin–gold (10 nm colloidal gold) (S9059), endothelial cell growth supplement (ECGS), basic fibroblast growth factor (bFGF), Megacell® DMEM (high glucose) cell culture medium, collagenase type II, gelatin, L-polylysine (MW 30–70 kDa), rabbit anti-human VIII factor IgG and 4′,6-Diamidino-2-phenylindole (DAPI), from Sigma company (Saint Louis, MO, USA); plastic cell culture dishes, plates and flasks, from Corning Incorporation (NJ, USA); fetal bovine serum (FBS), from Gibco (USA); fluorescein isothiacyanate (FITC)-conjugated goat anti-rabbit IgG, from Wuhan Boster Biological Technology Ltd., China; 3-(4,5-dimethylthiazol-2-yl)-2,5-diphenyltetrazolium bromide (MTT), from Sino-American Biotech (China); cellulose dialysis bag (cutoff molecular weight 14 kDa), from Pharmacia Company. Double distilled water was purified using a Millipore Simplicity System (Millipore, Bedford, USA). All the other chemicals were analytical reagent grades and used without further purification.

The animals used for the experiment were treated according to protocols evaluated and approved by the ethical committee of the University.

2.2. Copolymer synthesis and characterization

The MPEG–PLA and maleimide-polyethyleneglycol–poly(lactic acid) (maleimide-PEG–PLA) diblock copolymers were synthesized by ring opening polymerization according to our previous work [22]. In brief, a predetermined amount of MPEG or maleimide-PEG and D,L-lactide were placed in a dried round-bottomed bottle connected with a vacuum joint. In both cases, an appropriate amount of stannous octate was added as a solution in dried toluene. The reactants were dried under reduced pressure at 70 °C for 1 h, and then the reaction was proceeded under vacuum at 160 °C for 4 h. The cooled product was dissolved in dichloromethane, recovered by precipitation into an excessive mixed solvent of ethyl ether and petroleum ether. The precipitant was redissolved in acetone and precipitated into excessive water, with the purified copolymers dried in a vacuum oven at 40 °C for 24 h and then stored in a desiccator under vacuum.

The two copolymers were analyzed by ^{1}H and ^{13}C NMR spectroscopy at room temperature using a Varian Mercury Plus 400 MHz (USA) and with deuterochloroform as the solvent [23].

2.3. Preparation of CBSA–NP and BSA–NP

2.3.1. Pegylated nanoparticle (NP) preparation

Nanoparticles made of a blend of MPEG–PLA and maleimide-PEG–PLA were prepared through the emulsion/solvent evaporation technique according to the procedure described elsewhere [21]. Fifty microliters of water was emulsified by continuous sonication (30 s) on ice using a probe sonicator (JY92-II sonifier cell discruptor, Xinzhi Biotech Co., China) at 160 W in 1 ml of dichloromethane solution containing MPEG–PLA (24.0 mg/ml) and maleimide-PEG–PLA (2.4 mg/ml). This primary emulsion was then intermissively emulsified by sonication (30 s) at 160 W on ice in 2 ml of a 1% sodium cholate aqueous solution. The w/o/w emulsion obtained was diluted into 38 ml of a 0.5% sodium cholate aqueous solution under rapid magnetic stirring. After 1 min, dichloromethane was evaporated at low pressure and at 40 °C using a Büchi Rotavapor R-200 and Heating Bath B-490 (Germany). Nanoparticles were then centrifuged at 14,000 rpm with a TJ-25 Beckman Coulter TM Centrifuge equipped with AT-14-50 rotor (USA) at 4 °C for 45 min. After discarding the supernatant, they were resuspended in 0.5 ml of a 0.01 M HEPES buffer (containing 0.15 M NaCl and 0.1 mM EDTA, pH 7.0).

The preparation of nanoparticles loaded with 6-coumarin was the same as that of blank nanoparticles, except that 15 μl 6-coumarin (1 mg/ml stock solution in dichloromethane) was additionally added to dichloromethane containing copolymers before primary emulsification.

2.3.2. Preparation of CBSA

Cationic albumin was prepared from bovine serum albumin (BSA) as previously described [12]. Briefly, 250 ml 0.9 M ethylenediamine was slowly added to 4 ml 50% (m/v) BSA while being stirred and pH was adjusted to 4.75. Then, 360 mg EDAC was added, and the mixture was stirred at room temperature for 2 h.

The reaction was terminated by addition of 1.3 ml of 4 M acetate buffer (pH 4.75). The solution was concentrated in protein concentrator to a final volume of 25 ml, extensively dialyzed against double distilled water and finally freeze-dried. BSA and CBSA were characterized by SDS-PAGE and by isoelectric focusing (IEF).

2.3.3. CBSA–NP and BSA–NP preparation

CBSA was thiolated using 2-iminothiolane (Traut's reagent) [4]. CBSA was dissolved in 0.15 M Na-borate buffer/0.1 mM EDTA (pH 8.5) followed by the addition of Traut's reagent in the same buffer with a 40:1 molar ratio CBSA to 2-iminothiolane. After incubation at room temperature for 60 min, the buffer was exchanged with 0.01 M HEPES (containing 0.15 M NaCl and 0.01 mM EDTA, pH 7.0) using Amicon TM Ultra-4 concentrator tube with ultrafilter membrane (cutoff molecular weight 30 kDa). Ellman's reagent was used to determine the extent of thiolation [24].

The thiolated CBSA was then mixed with nanoparticles at a thiolated CBSA:maleimide ratio of 1:1. The volume of mixture was 1 ml and the conjugation of the CBSA to the blank or nanoparticle loaded with 6-coumarin was performed overnight on a rotating plate set at a low speed. The reaction mixture was then applied to a 1.6×20 cm Sepharose CL-4B column and was eluted with 0.01 M PBS buffer (pH 7.4). The milky CBSA–NP fractions were visually identified and collected, and the nanoparticle concentration was determined by turbidimetry.

The thiolation of BSA, conjugation to nanoparticle and separation of BSA–NP were the same as those of CBSA–NP; the ratio of thiolated CBSA to maleimide was 1:1.

2.4. CBSA–NP characterization

2.4.1. Morphology, particle size and surface charge

The mean (number based and weight based) diameter and zeta potential of the nanoparticles were determined by dynamic light scattering (DLS) using a Zeta Potential/Particle Sizer NICOMP TM 380 ZLS (PSS.NICOMP PARTICLE SIZE SYSTEM, Santa Barbara, USA). The morphological examination of nanoparticles was observed by transmission electron microscope (H-600, Hitachi, Japan).

2.4.2. Dry weight content and turbidimetry measurements

Three batches of nanoparticles were prepared as described above, except that nanoparticle solution medium was replaced with water after preparation. Half of nanoparticles were used as the standard nanoparticle suspension for the calibrating turbidimetry method; the other half were used for dry-weight content determination. The preparation of dry-weight sample was based on the procedure reported [21]. Nanoparticle concentration was measured by turbidimetry measurements at 350 nm using UV 2401 spectrophotometer (Shimadzu, Japan), as the 6-coumarin had the absorption at 400 nm. The method was calibrated using the nanoparticle preparations, the dry-weight contents of which were determined. The turbidity versus concentration ranged from 0.1892 to 0.7568 mg/ml dry-weight content ($A_{350} = 1.2025C - 0.0700$, $r = 0.9997$).

2.4.3. X-ray photoelectron spectroscopy (XPS)

NP and CBSA–NP samples were lyophilized using ALPHA 2-4 Freeze Dryer (0.070 Mbar Vakuum, − 80 °C, Martin Christ, Germany). NP, CBSA–NP and the mixture of maleimide-PEG–PLA:MPEG–PLA (1:10) were analyzed to determine the surface composition of C, O and N with XPS. The analysis was performed on a PHI 5000 C ESCA system (USA) using Al K α X-rays ($h\upsilon$ 1486.6 eV) and an electron take-off angle of 45°. For each sample we recorded a single survey scan spectrum (0–1000 eV) and several narrow scans for C1s, O1s and N1s. The analyser was used in fixed transmission mode with pass energies of 50 eV or 20 eV for the survey or narrow scans, respectively, and acquisition and analysis of data were performed by a PHI 5000 C ESCA system. Peak curve fitting was carried out by means of the software provided by the XPSPEAK Version 4.0. The atomic composition for each sample was calibrated from the C1s, O1s and N1s envelope intensities divided by C1s, O1s and N1s sensitivity factor of 0.25, 0.66 and 0.42, respectively. Chemical shifts were referenced to hydrocarbon at 285 eV [23,25,26].

2.4.4. Electron microscopy of gold-labeled CBSA–NP

To make further confirmation of the covalent conjugation of CBSA with pegylated nanoparticles, the immuno-gold staining technique was adopted. As CBSA can bind negatively charged glycoproteins

with sialic acid residues on the luminal side and heparan sulfates on the abluminal side of the brain capillary endothelial plasma membrane to initiate AMT [3], we used the heparin–biotin as the "first antibody" to combine CBSA part around the surface of CBSA–NP to form NP–CBSA/heparin–biotin complex, and used the streptavidin–gold as the "second antibody" to combine with the biotin part of the NP–CBSA/heparin–biotin complex to form NP–CBSA/heparin–biotin/streptavidin–gold complex. If the pegylated nanoparticles were conjugated with CBSA, they would be stained with the colloidal gold.

There were two steps for gold staining. First, 10–20 μg CBSA–NP in 0.01 M PBS solution was incubated with 100 μl 1 mg/ml heparin™–biotin sodium salt in 0.01 M PBS (containing 0.15 M NaCl, 0.5% BSA and 12% glycerol, pH 7.0) at 37 °C for 1 h with shaking at 70 rpm. The heparin–biotin bound to the CBSA–NP was separated from unbound conjugate by passing through a 0.5 × 10 cm column of Sepharose CL-4B and then collected. After that, NP–CBSA/heparin–biotin fraction was incubated with 100 μl streptavidin–gold (10 nm colloidal gold, 1:10 diluted with 0.15 M NaCl, 0.01 M PBS, 0.5% BSA, 12% glycerol, pH 7.0) for 1 h at 37 °C with shaking at 70 rpm. The gold-labeled CBSA–NP was separated from unbound gold by another passing through a 0.5 × 10 cm column of Sepharose CL-4B. In order to validate the specificity of this immuno-gold stain method, two control groups were set up. The first control group was to use CBSA–NP to only perform the second step, during which CBSA–NP was allowed directly to incubate with streptavidin–gold followed by Sepharose purification procedure. The second control group was intended to use CBSA-unconjugated nanoparticle (NP) to perform the two steps.

All three nanoparticle groups were negatively stained with 2% (w/v) phosphotungstic acid solution (pH 7.0) and deposited on a 200 mesh formvar-coated copper grid. Morphology observation was performed using a Hitachi H-600 transmission electron microscope (Japan) at 80 kV. Negatives, taken at a 120,000 magnification, were scanned and enlarged in Adobe Photoshop 6.0.

2.4.5. Determination of the loading efficiency

To determine the 6-coumarin content, CBSA–NP and BSA–NP were dissolved in methanol with the 6-coumarin determined by HPLC analysis [27]. A 20 μl diluted sample was injected in the system. The HPLC system (Shimadzu Scientific Instrument Inc., Japan) consisted of a pump (LC-10ATVP) and a fluorescence detector (Model RF-10AXL, Ex 465 nm/Em 502 nm). With a Dikma Diamonsil C18 (5μm, 200 mm × 4.6 mm) column, the separations were achieved in methanol:20 mM ammonium acetate buffer (93:7, pH 4.0) mobile phase with a flow rate of 1.2 ml/min and column temperature of 35 °C.

The 6-coumarin loading efficiency (DLE) was calculated by the following equation:

$$\mathrm{DLE}\% = \frac{6 - \text{Coumarin concentration in nanoparticle solution}}{\text{Nanoparticle concentration in the same solution}} \times 100\%.$$

2.5. In vitro release of 6-coumarin from CBSA–NP

The release test of 6-coumarin in vitro was performed by incubating 1.0 ml of about 2 mg of 6-coumarin-loaded CBSA–NP in a dialysis bag and immersed in 19.0 ml pH 4 and 7.4 PBS, which is present in the endo-lysosomal compartment and is the physiologic pH, respectively. The entire system was kept at 37 °C with shaking at 100 rpm. Samples (1.0 ml) were withdrawn from the medium and same volume of fresh dissolution medium was added. Samples were lyophilized and then reconstituted in 1 ml methanol [28]. The amount of 6-coumarin in each of the release samples was analyzed by HPLC method described above. Care was taken to protect the samples from light throughout the experimental procedure.

2.6. In vitro uptake of CBSA–NP and BSA–NP loaded with 6-coumarin by brain capillary endothelial cell (BCEC)

2.6.1. Isolation of brain capillaries and primary culture of BCECs of rat

The method of the primary culture was adopted and modified according to previously described techniques [29–31]. The brain cortices of SD rats 1–3 days after birth were dissected free of meninges and minced. The dissection was done in Hank's balance salt solution (HBSS) on ice. The homogenate was digested in 0.05% trypsin for 30 min at 37 °C. Subsequently,

DMEM supplemented 10% FBS was added to the trypsin solution, and the homogenate was centrifuged at 1000 rpm for 5 min. The supernatant was discarded, the digested homogenate was resuspended by adding 15% dextran solution (1:1, v/v), followed by centrifugation at 2000 rpm for 20 min. The pellet was resuspended with HBSS and filtered through a 150-μm stainless steel mesh sieve. The filtrate was collected. Following the second filtration through a 75-μm stainless steel mesh sieve, the capillaries were collected on the sieve, which were secondly digested in 1 mg/ml collagenase type II for 30 min at 37 °C. Subsequently, DMEM supplemented 10% FBS was added to the collagenase solution, and the supernatant was discarded after centrifugation at 1000 rpm for 5 min. The capillaries were resuspended by adding 1 ml DMEM containing 20% FBS, penicillin (100 U/ml) and streptomycin (100 mg/ml), and seeded onto a 35-mm-diameter culture dish coated with 1% gelatin.

On the 4th day, the endothelial cells began to migrate out from the capillaries, forming colonies. ECGS and bFGF were added at the final concentration of 0.2 mg/ml and 10 ng/ml, respectively. The culture medium was changed every 3 days. On the 10th day, the colonies grew larger, and the five largest endothelial colonies were retained and the others were scraped by rubber policeman. The dish was rinsed by PBS for three times, and trypsinized to subpassage onto another 35-mm-diameter culture dish coated with 1% gelatin. The culture medium was changed every 3 days. Seven days later, the cells reached confluency, and subpassage at the split ratio of 1:4. The BCECs used for nanoparticle uptake study were passage 3–7.

2.6.2. Immunocytochemistry of BCEC

The cells cultured on glass cover slips coated with L-polylysine were fixed with 4% paraformaldehyde at room temperature for 20 min. The cells were washed with PBS for three times, and permeated with ice-cold acetone at −20 °C for 7 min. The rinsed cover slips were incubated with 10% normal goat serum for 30 min in a humidified chamber at 37 °C. Immunostaining was carried out as previously described [32]. Afterwards, the cover slips were incubated in 37 °C with rabbit anti-human factor VIII-related IgG diluted 1:200 in PBS for 1 h. Rinsed again, the cover slips were exposed to FITC-conjugated goat anti-rabbit IgG diluted 1:40 in PBS at 37 °C for 1 h, and rinsed for the third time before being mounted in Dako Cytomation fluorescent mounting medium (Dako, USA). The slides were examined with Zeiss LSM 510 (Germany).

2.6.3. Quantitative analysis of 6-coumarin-loaded CBSA–NP and BSA–NP uptake

BCECs were seeded at a density of 10^5 cells/cm^2 onto 24-well plates. Three or four days later, the cells were used for the quantitative analysis of nanoparticle uptake [27]. A stock suspension of CBSA–NP and BSA–NP (2 mg/ml) in HBSS was prepared and sonicated for 10 min over a SB 2200-T water bath sonicator (Branson, Shanghai, China). Different dilutions of nanoparticles in the concentration range of 10–600 μg/ml were prepared from the stock in HBSS. Pre-incubated with HBSS for 15 min, the medium was replaced with the suspension of nanoparticles and incubated for 1 h at 4 °C and 37 °C, respectively. In a separate experiment, to study the effects of incubation time on nanoparticle uptake, the medium was replaced with 1 ml 100 μg/ml suspension of nanoparticles in HBSS per well and the plate was incubated for 15 min, 30 min, 1 h, 2 h and 4 h at 37 °C. At the end of the incubation period, the cells were washed with ice-cold uptake buffer, then with acid buffer at 4 °C for 5 min (consisting of 120 mM NaCl, 20 mM sodium barbital and 20 mM sodium acetate, pH 3), and washed again with ice-cold uptake buffer [12]. Subsequently, the cells were solubilized in 400 μl 1% Triton X-100 and 20 μl of the cell lysate from each well was used to determine the total cell protein content using BCA protein assay (Shanghai Shenergy Biocolor Bioscience and Technology Co., Ltd, China). A standard curve was obtained with BSA solution. The remainder of the cell lysates were lyophilized and used for HPLC analysis of 6-coumarin. The extraction of 6-coumarin was according to the optimized procedure [27]. A standard curve for nanoparticles was constructed by suspending different weight concentrations of nanoparticles (1.25–550 ng/ml) in 1% Triton X-100 followed by lyophilization and extraction of 6-coumarin in methanol. The standard was run at the same time and treated in a similar way as samples from the cell culture experiments. The uptake of nanoparticles by BCECs was calculated from the standard curve and expressed as the amount of nanoparticles (μg) taken up per mg cell protein.

2.6.4. Fluorescent microscopy of nanoparticle binding/uptake by BCECs

BCECs were seeded at a density of 10^4 cells/cm^2 in the polylysine-coated glass cover slip. Three or four days later, the cells were applied to the qualitative analysis of nanoparticle uptake [27,28]. Equilibrating with HBSS for 15 min, the cells were incubated with 6-coumarin-loaded CBSA–NP and BSA–NP suspensions (300 μg/ml in HBSS, pH 7.4) for 0.5, 1 and 2 h at 37 °C, respectively. At the end of the experiment, the cells were washed four times with PBS and fixed by 4% paraformaldehyde for 20 min. Then, they were washed three times with PBS, mounted in Dako fluorescent mounting medium and observed under Nikon UFX-II fluorescent microscope (Japan).

2.7. Distribution of 6-coumarin-labeled CBSA–NP and BSA–NP into the mouse brain

6-Coumarin-labeled CBSA–NP and BSA–NP were injected into the caudal veins (dose 60 mg/kg) of mice, respectively. Thirty minutes later, the animals were anaesthetized with ether and the blood was cleared from the circulation by transcardiac perfusion (15 ml 0.9% NaCl followed by 30 ml 4% paraformaldehyde). The brains were removed, about 1 cm thickness of coronal section samples post optic chiasma were collected and fixed in 4% paraformaldehyde overnight. After that, samples were placed in 15% sucrose PBS solution for 12 h, and then replaced with 30% sucrose for 24 h. Following this, the samples were embedded in Tissue Tek® O.C.T. compound (Sakura, USA) and frozen at − 60 °C in isopentane [33]. The frozen sections of 5 μm thickness were stained with 1 μg/ml DAPI for 10 min at room temperature. After PBS washing, the sections were prepared with a cryotome Cryostat (Leica, CM 1900, Germany), mounted in Dako fluorescent mounting medium and examined under the fluorescence microscope (Olympus, Japan).

2.8. In vitro cytotoxicity of CBSA–NP on BCECs

The determination of cell viability is a common assay to evaluate the cytotoxicity of CBSA–NP by the MTT assays in vitro [34]. BCECs were seeded onto 96-well plates at a density of 10,000 cells/well and cultured in 100 μl of cell growth medium for 2 days in the CO_2 incubator. After pre-incubation with HBSS, the medium was replaced with CBSA, NP and CBSA–NP samples to give a concentration of 0.025 to 8.0 mg/ml in HBSS (pH 7.4). After 4 h of incubation at 37 °C, the nanoparticles were replaced with 100 μl of MTT (0.5 mg/ml in HBSS) solutions, and the cells incubated for a further 3 h at 37 °C. The test solution was decanted, and 150 μl of DMSO was added to solubilize the cells. The resultant solutions were measured using a ELX800 Universal Microplate Reader (BIO-TEK Instruments, Inc., USA) at λ_{570} test wavelength and λ_{630} reference wavelength. Cell viability was expressed as percentage of absorbance in comparison with that of the control, which comprised the cells without exposure to the nanoparticles. The experiments were performed in triplicates. The IC_{50} and IC_{20} represented the respective concentrations at which 50% and 20% of cell growth were inhibited.

3. Results and discussion

3.1. Characterization of MPEG–PLA and maleimide-PEG–PLA

The two copolymers were synthesized by ring open polymerization of D,L-lactide initiated by the hydroxyl group of MPEG and maleimide-PEG, respectively. Chemical shifts in ppm (δ) were determined using the chloroform signals at 7.26 ppm (^{1}H) or at 77.00 ppm (^{13}C). ^{1}H and ^{13}C NMR spectra (Fig. 2) demonstrated the peaks at 1.65 (^{1}H) and 16.67 ppm (^{13}C) belonged to methyl group (–CH_3) while 5.20 (^{1}H) and 68.98 ppm (^{13}C) referred to methine group (–CH–) of PLA segment. The methene group (–CH_2–) of PEG segment appeared at 3.65 (^{1}H) and 70.56 ppm (^{13}C), and the carbonyl carbons of (C=O), at 169.52 ppm (^{13}C). The low signal peak integral at 6.65 ppm (^{1}H) corresponding to the maleimide protons was detected to prove the preservation of the maleimide function in the synthesized maleimide-PEG–PLA [21,23]. No other peaks were detected, which indicated the high purity of the two copolymers. From the ^{1}H ratio of peak area at 5.20 and 3.65 ppm, the average molecular weight ratios of maleimide-PEG to PLA and MPEG to PLA of the two synthesized copolymers were determined to be 3400:40,600 and 3000:40,100, respectively, suggesting that molecular weights of maleimide-PEG–PLA and MPEG–PLA were 44,000 and 43,100.

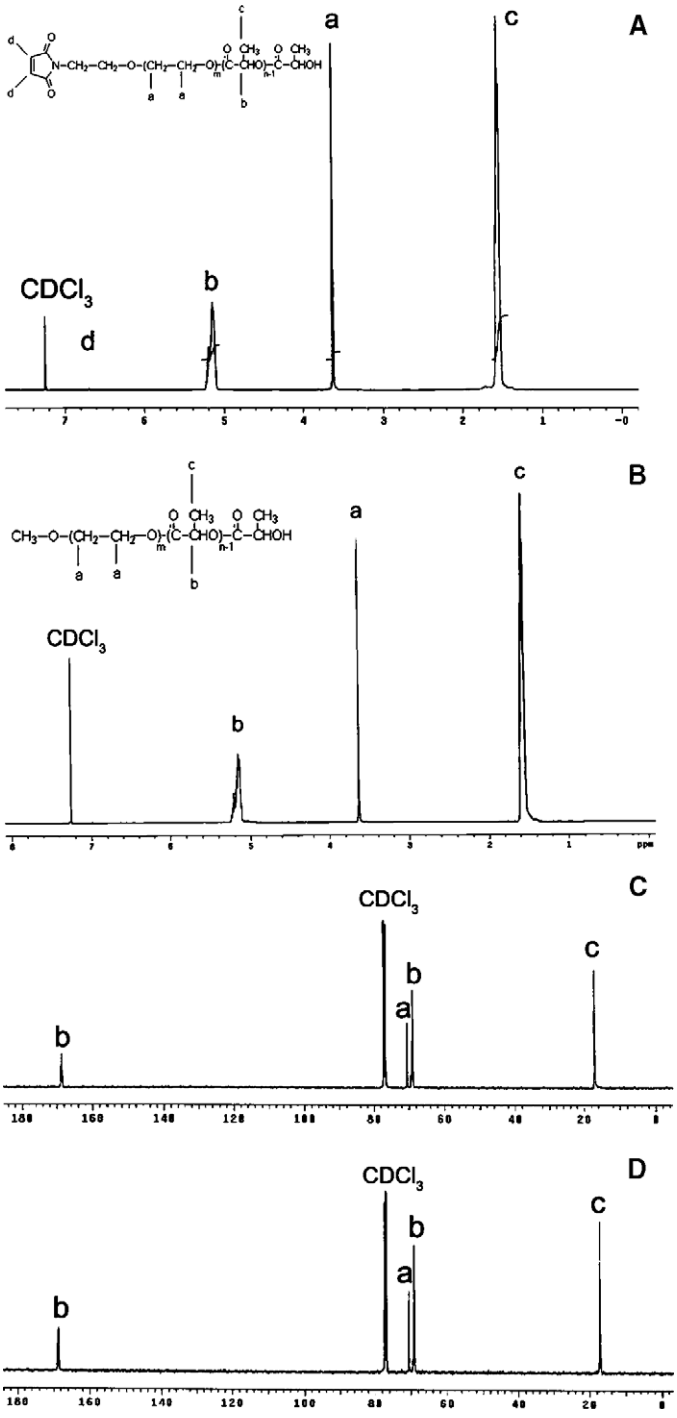

Fig. 2. (A) and (B) represent formula and ^{1}H NMR spectrum of maleimide-PEG–PLA and MPEG–PLA copolymers in deuterochloroform, respectively; (C) and (D) represent ^{13}C NMR spectrum of maleimide-PEG–PLA and MPEG–PLA copolymers in deuterochloroform, respectively.

3.2. Characterization of CBSA–NP and BSA–NP

The cationization degree of BSA was optimized by adjusting the amount of EDAC. IEF showed that the p*I* of CBSA had a shift from 4 to 8–9 (Fig. 3A), while the molecular weight did not change in comparison with that of BSA, i.e. approximately 66 kDa according to the SDS-PAGE results and only a little amount of dimer was depicted (Fig. 3B). This mild cationization procedure needs to be controlled so as to avoid higher molecular weight aggregates [35]. Furthermore, as a favorable brain targetor, it suggested that for mildly cationized albumin, p*I* should probably be between 8 and 9 [3]. The ratio of CBSA:2-iminothiolane was adjusted to 1:40 according to the previous report [4], which provided a thiolation degree of an average of about 1.5 mol thio-group per mol CBSA.

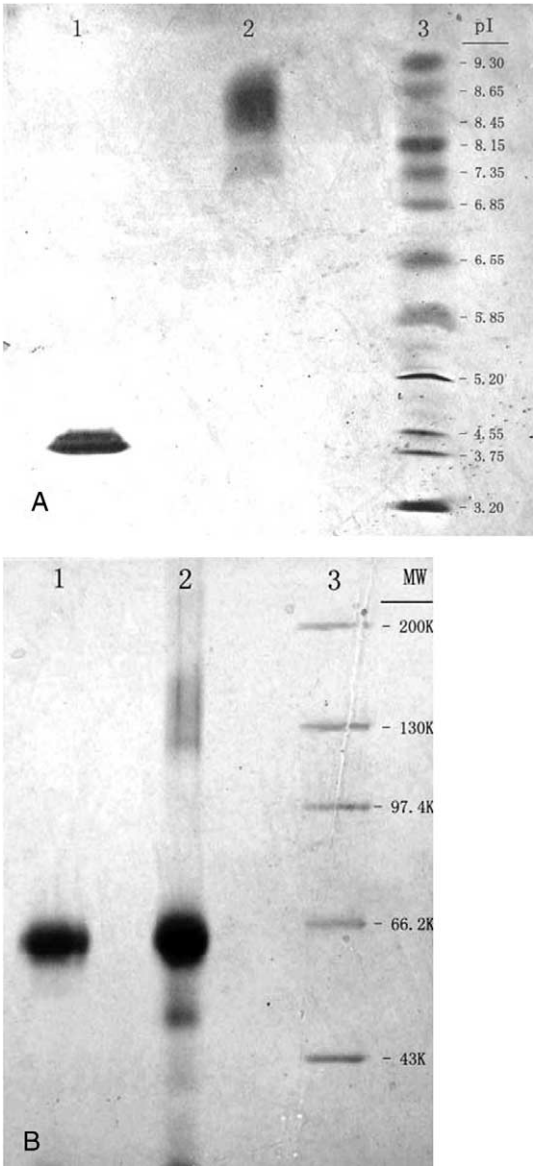

Fig. 3. (A) and (B) represent IEF and SDS-PAGE diagram of native BSA (lane 1), CBSA (lane 2) and marker (lane 3), respectively.

The double emulsion technique chosen here provided the nanoparticle forming the inner aqueous phase, which could dissolve hydrophilic drugs, including small molecules, proteins and gene drugs [36,37]. Due to the phase separation, the hydrophilic PEG chains oriented themselves toward both aqueous phases of the nanoparticles during the hardening procedure, thus causing some of maleimide-PEG chains to move toward the inner phase [21]. Therefore, some of the bifunctional PEG did not extrude out of the nanoparticles and could not conjugate with the thiolated CBSA. The OX26-conjugated pegylated nanoparticles showed the mixture ratio of maleimide-PEG–PLA and MPEG–PLA when preparing NPs was optimized at 1:30 [21]. However, the different brain delivery mechanism between CBSA–NP and OX26-conjugated nanoparticles is their different transport process between AMT and RMT. Bickel et al. reported that the main difference between AMT and RMT lies in the affinity and capacity of these two pathways. AMT is characterized by lower affinity and higher capacity compared with RMT [3]. If an AMT process is initiated by CBSA, more CBSA should be designed to conjugate nanoparticle's surface than OX26. Accordingly, we adjusted the mixture ratio of maleimide-PEG–PLA and MPEG–PLA to 1:10, and the ratio of CBSA:maleimide group was 1:1 to allow full reaction to the surface maleimide group.

Most NPs and CBSA–NPs loaded or not with 6-coumarin were generally spherical and of regular size under the examination of TEM. The TEM of 6-coumarin-loaded CBSA–NP is shown in Fig. 4. The number-based average diameters of the five types of nanoparticles were about 80 nm, while their weight-based values were around 100 nm (Table 1). There was no significant difference of particle size between nanoparticles conjugated or not with CBSA and load-

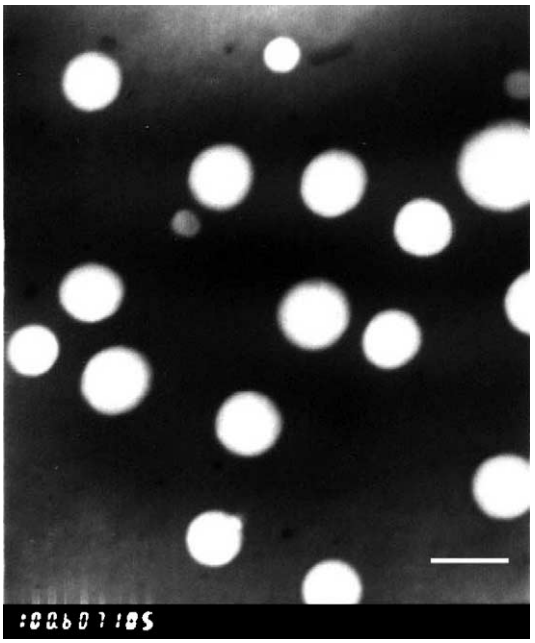

Fig. 4. Transmission electron micrograph of CBSA–NP negatively stained with phosphotungstic acid solution. The magnification bar is 100 nm.

ed or not with 6-coumarin, suggesting that neither the conjugation process with CBSA nor incorporation of the fluorescent dye influenced the particle size. Since the particle size is an important property that affects the endocytosis by the brain capillary cells, the size distribution was generally controlled under 200 nm in diameter not only for nanoparticles [21,33] but also for immunoliposomes [4–8,12]. Particles less than 200 nm were also found to prevent spleen filtering [38].

The zeta potential values of blank CBSA–NPs and NPs (Table 1) were around −10 mV. The still negatively charged zeta potential of CBSA–NP might not be contradictory to the adsorptive endocytosis of the nanoparticles, although cationic nanoparticles made by some cationic polymers such as chitosan resulted in positive zeta potential [39]. Because zeta potential is the difference in the electrical charge between the dense layer of ions surrounding the particles and the charge of the bulk of the suspended fluid surrounding this particle, it gives information about the overall surface charge of the particles. Therefore, the zeta potential of CBSA–NP was attributed to two factors: first, the PEG surface shielding effect on offsetting the negative charge of the PLA segments in the nanoparticle core; second, the CBSA surface amount and its cationization degree. Considering the first point, the increased zeta potential from about −30 mV of PLA nanoparticle of literature report [36] to −10 mV of our NP result demonstrated that the "brush" effect of surface PEG screening the negative charge of carboxyl end groups from PLA is significant. This is the predominant cause in influencing the zeta potential. Concerning the second point, the cationization degree of BSA was mild with CBSA p*I* value of 8–9. In addition, the surface amount of CBSA was little (surface nitrogen amount was only 0.9% of surface atomic composition C, O, N, see XPS analysis results below). So the positive charge contribution of surface CBSA was insignificant. This caused the zeta potential of CBSA–NP to be slightly increased compared with NP but still negative.

However, the negative zeta potential in response to overall surface charge of the particles does not reflect the local microenvironment surrounding each CBSA milieu on the nanoparticle's surface. In these local CBSA microenvironments, the net electrical charge might be speculated to be positive. Regarding this, it might be possible for CBSA protruding out side of the nanoparticle to electrostatically bind the negatively

Table 1
The particle size and zeta potential of NPs and CBSA–NPs loaded or not with 6-coumarin ($n=3$)

Nanoparticles	Mean size (mean ± SD, nm)		Size range (nm)		Zeta potential (mV)[a]
	Number based	Weight based	Number based	Weight based	
NP	83.5 ± 3.5	93.6 ± 2.5	48.2–115.8	73.9–106.9	− 9.36 ± 0.84
CBSA–NP	84.4 ± 3.0	95.2 ± 5.1	75.9–100.1	71.9–110.9	− 8.92 ± 0.65
6-Coumarin-loaded NP	80.4 ± 6.6	101.9 ± 1.8	60.9–100.3	85.8–116.7	− 16.81 ± 1.05
6-Coumarin-loaded CBSA–NP	82.1 ± 4.0	107.4 ± 6.0	68.8–95.1	87.9–129.2	− 12.19 ± 1.21
6-Coumarin-loaded BSA–NP	83.2 ± 4.4	108.7 ± 7.8	70.4–96.8	84.3–128.4	− 16.7 ± 0.86

[a] Measured in NaCl solution (10^{-3} M).

charged residues on BBB. It is not that the whole nanoparticle interacts with the anionic binding sites of brain capillaries, but that its surface CBSA undergoes AMT of CBSA–NP. This was structurally supported by our design of CBSA–NP, in which the molecular weight of maleimide-PEG part was chosen higher than MPEG so as to facilitate the maleimide function group to couple with CBSA and this targetor to protrude from MPEG corona to bind negatively charged residues on BBB. Our electron microscopy of specific gold staining of CBSA–NP proved that the surface CBSA can electrostatically bind the heparin residue (see electron microscopy result below), which is the component of AMT binding site in the wall of brain capillaries [3]. Furthermore, the fact that surface CBSA undergoes AMT of nanocontainer was also confirmed by the uptake of CBSA-conjugated pegylated liposome by cultured porcine brain microvessel endothelial cells and intact brain capillaries [12].

The zeta potentials of 6-coumarin-loaded nanoparticles were lower than that of the blank (Table 1) ascribed to part of the embedded PEG chains inside the matrix. Owing to 6-coumarin entrapment, the density of PEG "brush" was lower than that of the blank [36].

3.3. Surface analysis

From the XPS analysis, the survey scan of maleimide-PEG–PLA:MPEG–PLA (1:10) copolymers, NPs and CBSA–NPs provided quantitative data for surface atomic composition (Table 2). The surface nitrogen was only detected in the CBSA–NP sample with the value of 0.9% with regard to the total amount of C, O, and N atoms. There were a total of 4 peaks presented to achieve the best fit in the C1s envelope (Fig. 5). Peak 1 represented the carbon in C–C or C–H [25]. Peak 2 was generated by an ether environment ($–CH_2–CH_2–O–CH_2–CH_2–$) of chemical shift 1.8 eV in relation to the peak 1 environment. Peaks 3 and 4 corresponded to carbon of ester and carboxylate of chemical shifts 2.6 and 4.5 eV in relation to the peak 1 environment, respectively. The decomposition of the O1s envelope revealed the presence of two types of oxygen O=C at 532.0 eV and O–C at 533.3 eV (data not shown) [40]. Peak 5 corresponded to the N1s envelope at 399.5 eV with a low signal. The percentage compositions of these components are given in Table 2.

According to the chemical structures of the three kinds of samples, the nitrogen was ascribed to maleimide group of maleimide-PEG–PLA and CBSA. The scan of the nitrogen failed to detect the existence of N1s both on the maleimide-PEG–PLA:MPEG–PLA copolymers mixture and NPs, suggesting that the nitrogen contribution of maleimide group in XPS can be neglected. Since XPS determines the elemental and average chemical composition of the material at its surface in 5–10 nm depth and the detection limit of XPS is 0.1% [23], the detected N1s signal of CBSA–NP sample can exactly be attributed to CBSA on the nanoparticles surface. Since peak 2 at the binding energy 286.8 eV is regarded as the indicator of MPEG [23], the presence of PEG on the particle's surface can be confirmed by an increased C–O–C peak ratio of 21.7% and 30.4% of NPs and CBSA–NPs, respectively, compared with that of the maleimide-PEG–PLA:MPEG–PLA copo-

Table 2
The XPS analysis of maleimide-PEG–PLA:MPEG–PLA mixture (1:10), pegylated nanoparticles conjugated or not with CBSA

Sample	XPS elemental ratio (%)			XPS C1s envelope ratios (%)				XPS O1s envelope ratios (%)	
	C	O	N	C – C/C – H	C – O – C	C – O – C= O	O – C = O	O = C	O – C
				Binding energy (eV)					
				285.0	286.8	287.6	289.4	532.0	533.3
Copolymers	66.2	33.8	–	53.6	16.3	11.3	18.8	40.1	59.9
NP	64.0	36.0	–	53.0	21.7	8.0	17.3	51.7	48.3
CBSA–NP	56.3	42.8	0.9	40.5	30.4	11.0	18.1	44.1	55.9

–=Below the detection limit.
Copolymers=maleimide-PEG–PLA:MPEG–PLA mixture (1:10).

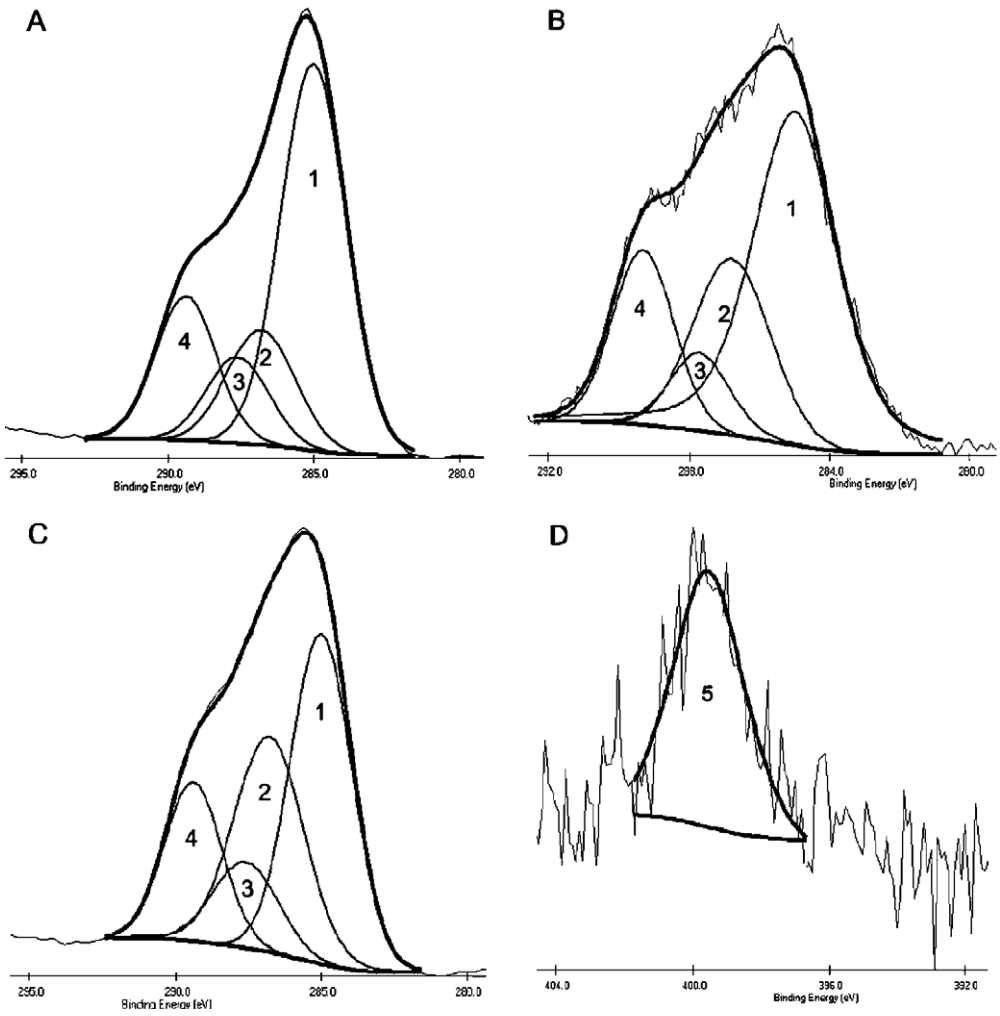

Fig. 5. Carbon C1s envelopes from XPS analysis of: (A) mixture of maleimide-PEG–PLA:MPEG–PLA mixture (1:10) copolymers, (B) pegylated nanoparticles unconjugated with CBSA (NP) and (C) CBSA–NP. Nitrogen N1s envelope from XPS analysis of (D) CBSA–NP.

lymers mixture (16.3%). This proved that the PEG "corona" layer existed.

3.4. Electron microscopy of gold-labeled CBSA–NP

It was visualized under TEM that the gold particles were stained around the nanoparticle's surface (Fig. 6A). This proved that the surface CBSA can bind the conjugate of heparin–biotin firstly and streptavidin–10 nm gold secondly. The gold was not detected because of lack of heparin–biotin (Fig. 6B). The NPs not conjugated with CBSA were not stained with gold (Fig. 6C). Both of negative control groups (Fig. 6B and C) can validate the specificity of this immunostaining procedure.

The rationale of this immuno-gold stain here is that the cationic protein can bind the anionic micro-domains on the luminal side consisting of negatively charged glycoproteins with sialic acid residues or the abluminal anionic binding sites containing heparan sulfates in the wall of brain capillaries [3,41]. This mechanism made us design the characterization approach by using CBSA on the nanoparticles to electrostatically bind heparin moiety of heparin–biotin conjugate, followed by conjugation of the streptavidin–gold through biotin/streptavidin binding process. The

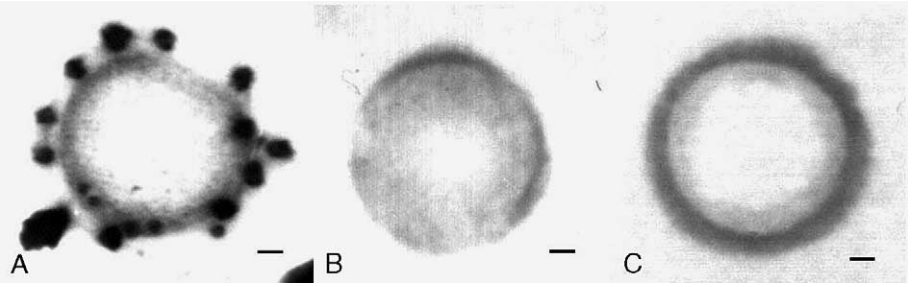

Fig. 6. Transmission electron micrograph of (A) CBSA–NP stained with heparin–biotin as the first " antibody " and 10 nm colloidal gold-labeled streptavidin as the second "antibody"; (B) CBSA–NP only stained with gold-labeled streptavidin; (C) NP stained with heparin–biotin as the first "antibody" and gold-labeled streptavidin as the second "antibody". The magnification bar is 10 nm.

positive staining results can also partially prove the functional targeting effects of CBSA–NP on the anionic binding sites of brain capillaries, although the XPS report showed only 0.9% nitrogen on the nanoparticle surface. Such amount may be enough.

3.5. Drug loading efficiency and in vitro release from CBSA–NP loaded with 6-coumarin

The DLE of 6-coumarin-loaded CBSA–NP and BSA–NP was $0.039 \pm 0.003\%$ and $0.038 \pm 0.004\%$, respectively. However, such amount of dye was enough to be detected qualitatively and quantitatively [27,28]. CBSA–NP loaded with 6-coumarin was characterized by the leaching of dye under different 0.1 M PBS conditions (pH 4.0 and 7.4). Approximately 0.48% of the dye was released from the CBSA–NP in pH 4.0 compared with about 0.72% released in pH 7.4 in 72 h when the sinking condition was assured (Fig. 7). The data were consistent with those of the previous report [28]. The relative inertia of the 6-coumarin encapsulated in CBSA–NP guaranteed that the dye was not released under the physiological condition or in the acidic endo-lysosome compartment. Labhasetwar et al. reported 6-coumarin had the advantage over other fluorescent dyes, which showed pH-dependent solubility such as rhodamine. When rhodamine loaded nanoparticles were endocytosed in the endo-lysosome, the red dye was released, which could lead to an inaccurate intracellular pattern

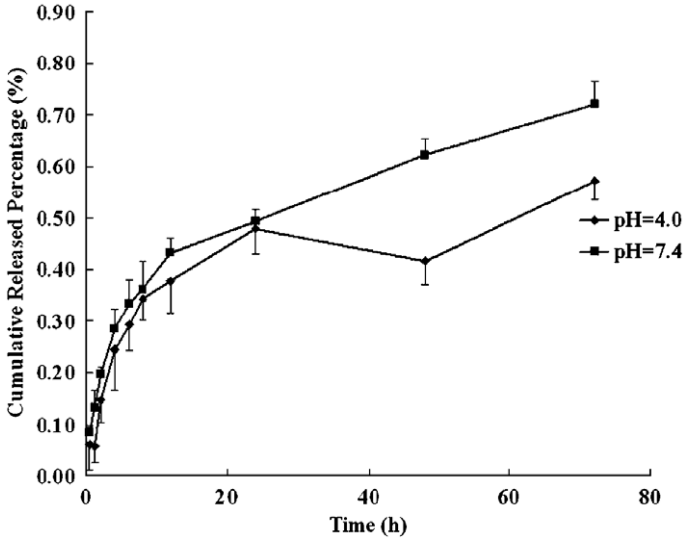

Fig. 7. In vitro release of 6-coumarin from CBSA–NP in 0.1 M PBS buffer of pH = 7.4 (square symbols) and 4.0 (diamond symbols).

[28]. The in vitro release from CBSA–NP ensured 6-coumarin to be an accurate probe for the nanoparticle's detection.

3.6. In vitro BCEC uptake of CBSA–NP and BSA–NP loaded with 6-coumarin

Five to six days after passage, BCECs reached confluency (Fig. 8A). When confluent, BCECs presented a small, tightly packed, nonoverlapping, contact-inhibited and polygonal shape, forming a monolayer, which was consistent with the literature [29–31]. BCECs were characterized by factor VIII (Fig. 8B). The cell purity was more than 95%, indicating that it was pure enough for the nanoparticle uptake experiment.

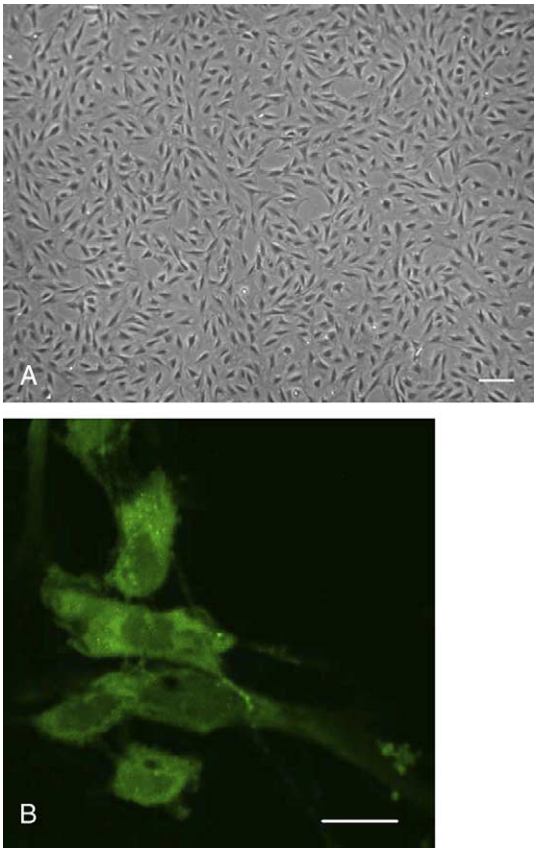

Fig. 8. (A) Five days after passage of the colonies formed in the primary culture, the BCECs reached confluence to form a monolayer of small, tightly packed, nonoverlapping, contact-inhibited cells (magnification bar is 100 μm.). (B) Immunocytochemistry of BCECs stained by rabbit anti-human VIII factor IgG as first antibody, FITC-conjugated goat anti-rabbit IgG as second antibody (magnification bar is 20 μm).

The uptake of CBSA–NP and BSA–NP by BCECs was dependent on the incubation time within 4 h (Fig. 9A). At each time point, the uptake amount of the CBSA–NP was higher than that of BSA–NP, even about 2 times higher than that of BSA–NP at 240 min. The uptake amount of both CBSA–NP and BSA–NP under 37 °C incubation was much higher than under 4 °C incubation, suggesting that the uptake of both nanoparticles was temperature-dependant (Fig. 9B). The uptake of CBSA–NP and BSA–NP was also concentration-dependant. The concentrations of CBSA–NP and BSA–NP upon the reach of saturation uptake by BCECs at 37 °C for 1 h were both about 300 μg/ml, while CBSA–NP uptake amount was about twofold higher than that of BSA–NP.

Fluorescent microscopy of BCECs exposed to CBSA–NP and BSA–NP at the same concentration (300 μg/ml) demonstrated that the increase of fluorescent intensity in the cells correlated with increase in the time of incubation (Fig. 10). There was a significantly accumulated amount of dye of CBSA–NP in the cells compared with that of BSA–NP for 30, 60 and 120 min at 37 °C, respectively. It was previously proved that free dye released from PLGA nanoparticles accounted for only about 3% of the total uptake of the dye after 2 h of incubation [27]. Our in vitro release results also confirmed the relatively inertia of the 6-coumarin in the nanoparticles. Thus, 6-coumarin detected in the cells dominantly reflected the nanoparticles. As a result, more CBSA–NP was visualized to be uptaken than BSA–NP.

Due to the saturable, time-, temperature- and concentration-dependant uptake behavior by BCECs, the nanoparticle's uptake can be considered as active endocytosis. Panyam and Labhasetwar used the 6-coumarin as the fluorescent probe to investigate the dynamics of endocytosis and exocytosis of poly(D,L-lactide-co-glycolide) nanoparticles in vascular smooth muscle cells in vitro. Their results proved that the nanoparticles could be transported in part through nonspecific receptor mediated endocytosis and in part through fluid-phase endocytosis [42]. As the uptake of CBSA–NP was enhanced, an additional endocytosis mechanism may be involved in CBSA–NP. On the other hand, the previous study provided evidence for much more FITC-labeled cationic CBSA

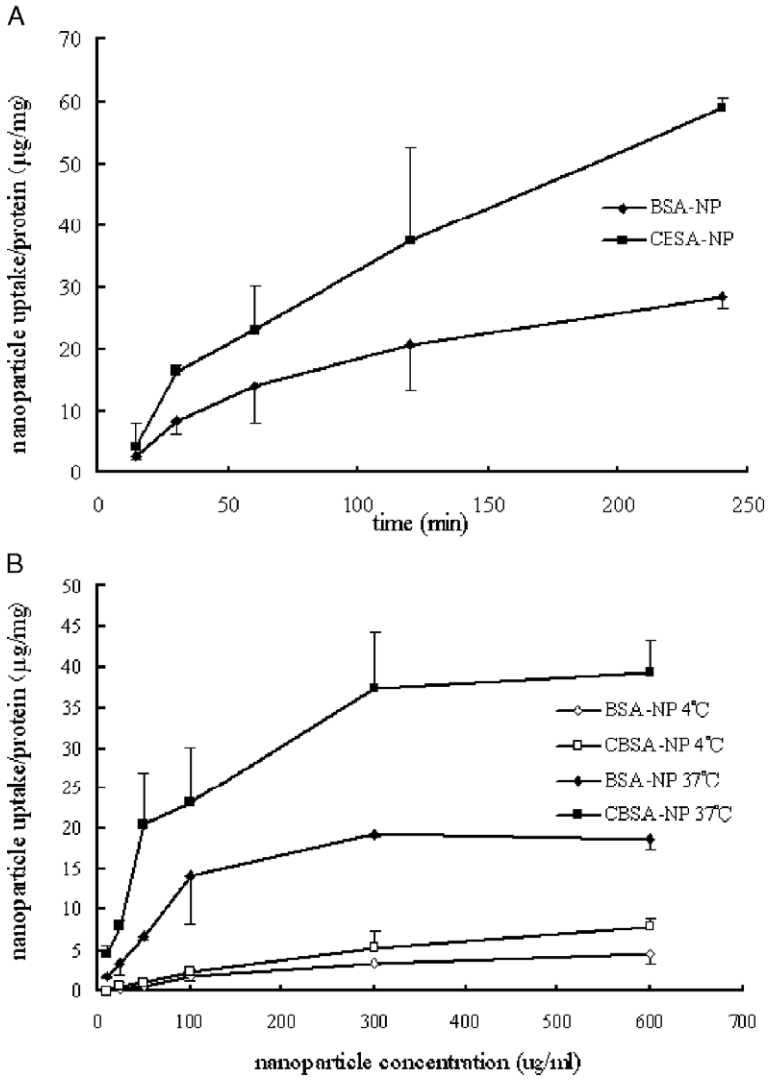

Fig. 9. (A) BCECs uptake 100 μg/ml CBSA–NP (square symbols) and BSA–NP (diamond symbols) at 37 °C incubation for different times, respectively; (B) BCECs uptake 10–600 μg/ml CBSA–NP (square and closed symbols) and BSA–NP (diamond and closed symbols) at 37 °C; 10–600 μg/ml CBSA–NP (square and opened symbols) and BSA–NP (diamond and opened symbols) at 4 °C incubation for 1 h, respectively.

taken up by porcine BCECs than FITC-labeled native BSA. The results derived from confocal laser scanning microscopy of the rhodamine-labeled CBSA-conjugated pegylated liposomes showed that it bound to cellular surfaces and exhibited time dependently higher intracellular accumulation in contrast to BSA-conjugated liposomes. This process could be blocked by specific cationic substances such as polylysine and caveolae-associated endocytosis specific inhibitor filipin, suggesting absorptive mediated endocytosis (AME) process during the endothelial cell uptake process with associated caveolin [12]. Therefore, the uptake of CBSA–NP can refer to AME initiated by CBSA.

In order to distinguish between surface binding and uptake by BCECs, the cells were washed with an acidic washing solution (pH 3) [12]. By protonation of carboxyl group, the number of negatively charged functions at the cell surface should be reduced so as to remove the electrostatically

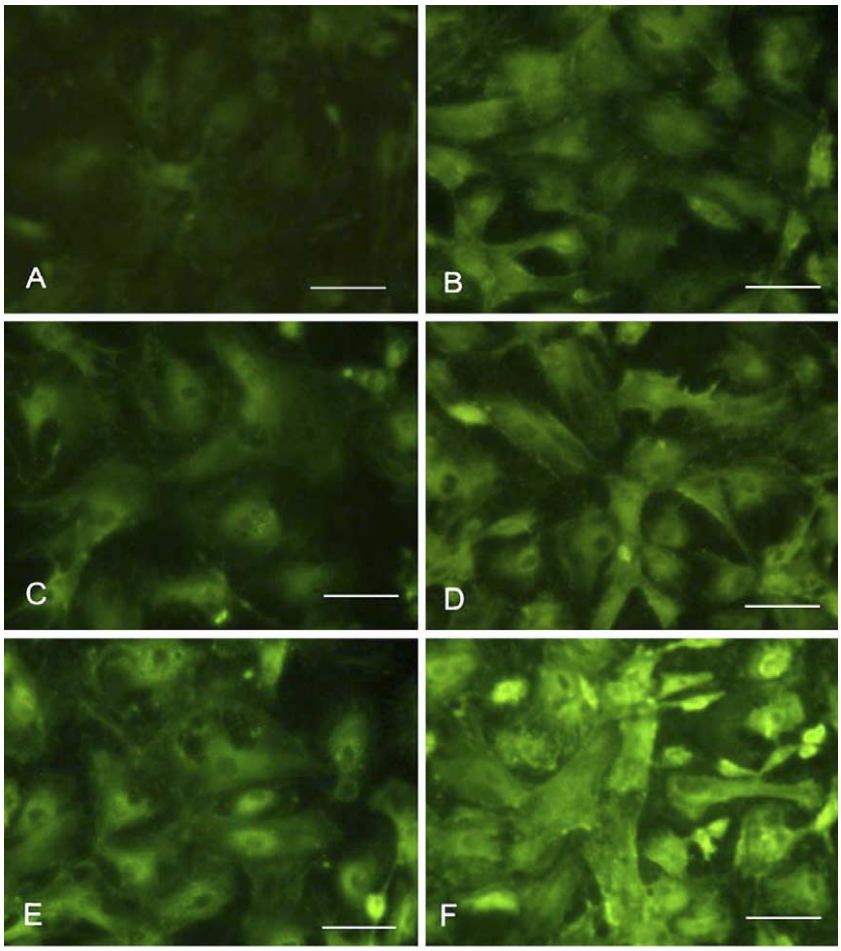

Fig. 10. BCECs uptake 300 μg/ml BSA–NP at 37 °C for 30 min (A), 60 min (C), 120 min (E) and 300 μg/ml CBSA–NP for 30 min (B), 60 min (D), 120 min (F), respectively. The magnification bar is 50 μm.

bound CBSA at the surface of plasma membrane [3,12]. But this was not applied in the qualitative observation experiment because acidic washing might influence the cellular morphology. Further experiment to distinguish the surface binding or uptake or both should be conducted using the confocal laser scanning microscopy with serial z-section of the cells.

3.7. Distribution of 6-coumarin-labeled CBSA–NP and BSA–NP in the mouse brain

Microscopic observation of coronal sections of the mouse brain showed that the fluorescent nanoparticles were localized mainly in the lateral ventricle, where CBSA–NP exhibited a greater distribution in choroid plexus than BSA–NP (Fig. 11A and B). And also much more green particles of CBSA–NP accumulated than those of BSA–NP in the third ventricle and its periventricular region (Fig. 11C and D).

Calvo et al. investigated the rat brain location of Fluorescent Fluorobrite™ nanoparticles coated with PEG-*n*-hexadecylcyanoacrylate (PEG-PHDCA) in 24 h [33]. The nanoparticles were mainly found in the ependymal cells and in the choroid plexus epithelial cells in lateral ventricle. Since the choroid plexus produces the cerebrospinal fluid (CSF), the nanoparticles' retention resulted from the secretion of CSF. This could explain why the negative control group (BSA–NP) was also found in this area, but with a

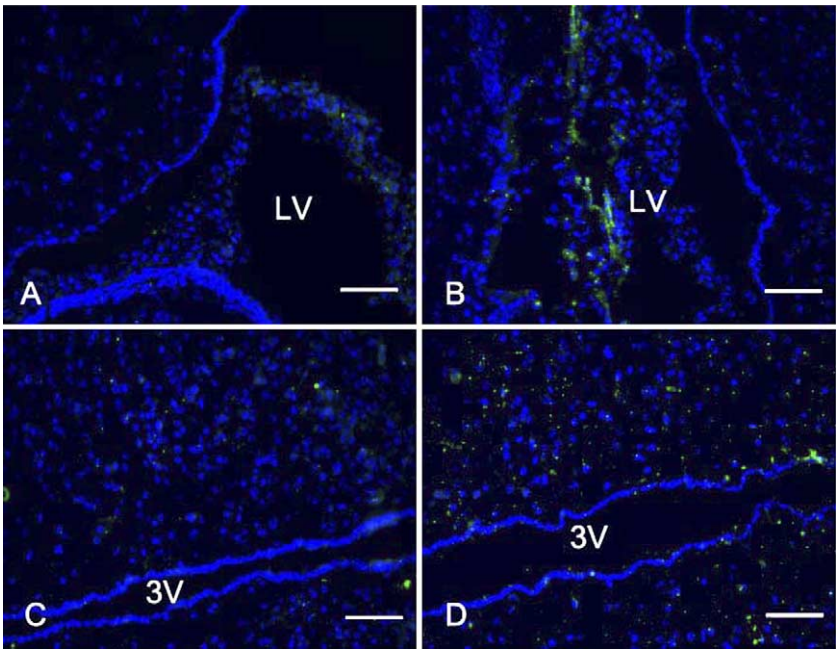

Fig. 11. Green dye distribution of 6-coumarin incorporated in BSA–NP (A) and CBSA–NP (B) in lateral ventricle and its periventricular region; distribution of BSA–NP (C) and CBSA–NP (D) in third ventricle and its periventricular region was visualized using the FITC filter 30 min after i.v. nanoparticles in mouse caudal vein at a dose of 60 mg/kg. The blue cell nuclei were stained with 1 μg/ml DAPI for 10 min visualized using UV filter. LV represents lateral ventricle, 3 V represents third ventricle. The magnification bar is 50 μm.

little amount. However, as systemically administered cationic albumin was rapidly transported into CSF [43], CBSA–NP tended to penetrate the choroid plexus into CSF 30 min after administration. Therefore, much more CBSA–NP was detected there than BSA–NP. The evidence that fluorescent CBSA–NP was highly distributed in the periventricular region of the third ventricle in contrast to BSA–NP indicated that the particles reached the brain parenchyma through the endothelial cells of BBB. This proved that the most likely transport mechanism is AMT process.

The transport physiology of CBSA was found as a BBB transport vector in experiments wherein the CBSA chimeric peptide was administrated in vivo. The cationic albumin binding β-endorphin resulted in rapid absorptive mediated endocytosis by the brain in vivo that greatly exceeded the uptake for native albumin binding β-endorphin [10]. Our results and data suggested that CBSA can be an effective brain targetor not only for the conjugation of non-BBB transportable neuropeptides but also for the coupling with nanocontainers.

Another interesting finding was that CBSA–NP accumulated in the periventricular region of the third ventricle where the hypothalamus is just located. As it is the regulation center to control autonomic functions including emotions, endocrine functions, homeostasis, motor functions, regulation of food and water uptake, regulation of sleep–week cycle, etc., the accumulation of CBSA–NP in this region encouraged us to deliver drugs for Parkinson's, obesity, sleep amelioration, wherein pharmacological target site is just there. For its inclination to reach such site, CBSA–NP could be designed as a hypothalamus drug delivery system. Nevertheless, further study should be done to evaluate its target efficiency and its long-circulating effects on promoting plasma AUC.

3.8. In vitro cytotoxicity of CBSA–NP on BCECs

MTT assay on BECEs viability showed that the cytotoxicity of CBSA, NP and CBSA–NP depended on their concentration ranging from 0.025 to 8 mg/ml (Fig. 12). From the viability–concentration curves, it can be derived that the IC_{20} of CBSA, NP and CBSA–

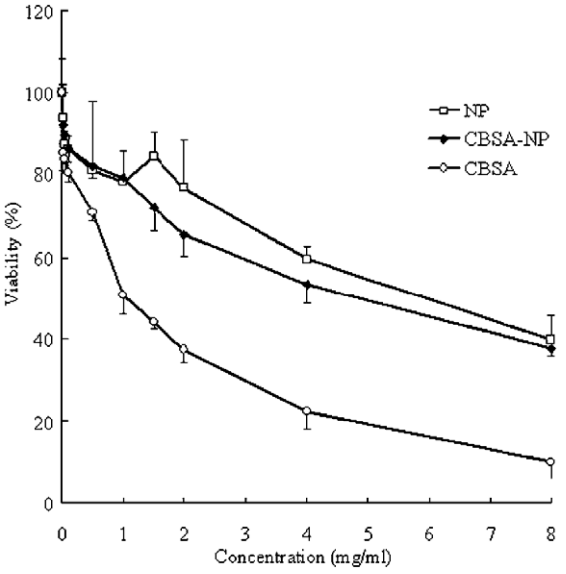

Fig. 12. In vitro cytotoxicity of NP (square and opened symbols), CBSA–NP (diamond and closed symbols) and CBSA (circle and opened symbols) on BCECs at concentration ranging from 0.025 to 8 mg/ml.

NP was about 0.1, 1.5 and 1 mg/ml, and IC_{50} was 1, 5.9 and 4.8 mg/ml, respectively. There was no significant difference between NP and CBSA–NP, while CBSA seemed a little bit cytotoxic.

The PLA polymers are generally accepted as low cytotoxicity with good biocompatibility, biodegradability and are currently being used in humans for resorbable sutures, bone implants and screws, and contraceptive implants [20,44,45]. Thus, NP was regarded as the "safety" control group. The slight difference of IC_{20} and IC_{50} between CBSA–NP and NP proved the relative "safety" of CBSA–NP to NP. As the IC_{50} of NP was only 5.9-fold higher than that of CBSA, we just concluded CBSA had a mild cytotoxicity on BCECs, and confirmed that cationic albumin with p*I* 8–9, not extreme cationization, had a mild cytotoxicity. These data can also indicate that the CBSA–NP below 1 mg/ml had little adverse effect on the BCECs viability, suggesting that the dose of in vitro BCECs uptake study (0.01–0.6 mg/ml) presented no toxicity. This is important because most of the cationic polymers and lipids, which are commonly used for gene transfection, have toxic effects on cells at a higher concentration [46]. Thus, the CBSA–NP is a promising carrier for brain gene delivery with low cytotoxicity. However, its long-term in vivo toxicity and immunogenicity should be further investigated.

4. Conclusion

This study for the first time presented a new brain drug delivery system with CBSA as a brain specific targetor covalently conjugated with the maleimide function group at the distal of PEG surrounding the nanoparticles. The surface characteristics of CBSA–NP were significantly different from those of the conventional cationic liposomes or nanoparticles since CBSA–NP had negative zeta potential, and the surface modification of CBSA with p*I* 8–9 showed less cytotoxity. The significantly increased uptake by BCECs compared with that by BSA–NP demonstrated that the AMT process initiated by CBSA existed. After a dose of 60 mg/kg CBSA–NP or BSA–NP injection in mouse caudal vein, the brain coronal section proved a higher accumulation of CBSA–NP in the lateral ventricle, third ventricle and periventricular region than that of BSA–NP.

The significant in vitro and in vivo results showed that CBSA–NP was a promising brain drug delivery carrier with low toxicity. Additionally, we for the first time used heparin–biotin and streptavidin–gold conjugates to detect CBSA at the surface of CBSA–NP. This specific immuno-gold staining technique cannot only prove the surface conjugation of CBSA, but predict its function, i.e. the ability of electrostatically binding the negatively charged residues on BBB as well.

Acknowledgements

This work was supported by National Natural Science Foundation of China (30472095), Nanotechnology Project of Shanghai Science and Technology Committee (0243nm067) and Innovation Foundation of Graduate Students of Fudan University. The authors acknowledge Dr. Chen Jiang, Dept. of Pharmaceutics, School of Pharmacy, Fudan University, China, for her precious suggestions on the experiment design. Thanks are given to Dr. Si-Shen Feng, Division of Bioengineering, National University of Singapore, Singapore, for his advice on XPS analysis and nano-

particle characterizations. Gratitude was also expressed to Dr. Vinod Labhasetwar, Department of Pharmaceutical Sciences, College of Pharmacy, Nebraska Medical Center, USA, for suggesting the application of the fluorescent dye, 6-coumarin incorporated in nanoparticles for cell uptake.

References

[1] W.M. Pardridge, Brain Drug Targeting, Cambridge University Press, Cambridge, 2001.
[2] W.M. Pardridge, Blood–brain barrier drug targeting: the future of brain drug development, Mol. Interv. 3 (2003) 90–105.
[3] U. Bickel, T. Yoshikawa, W.M. Pardridge, Delivery of peptides and proteins through the blood–brain barrier, Adv. Drug Deliv. Rev. 46 (2001) 247–279.
[4] J. Huwyler, D. Wu, W.M. Pardridge, Brain drug delivery of small molecules using immunoliposomes, Proc. Natl. Acad. Sci. U. S. A. 93 (1996) 14164–14169.
[5] N. Shi, W.M. Pardridge, Noninvasive gene targeting to the brain, Proc. Natl. Acad. Sci. U. S. A. 97 (2000) 7567–7572.
[6] N. Shi, Y. Zhang, C. Zhu, R.J. Boado, W.M. Pardridge, Brain-specific expression of an exogenous gene after i.v. administration, Proc. Natl. Acad. Sci. U. S. A. 98 (2001) 12754–12759.
[7] Y. Zhang, F. Calon, C. Zhu, R.J. Boado, W.M. Pardridge, Intravenous nonviral gene therapy causes normalization of striatal tyrosine hydroxylase and reversal of motor impairment in experimental parkinsonism, Hum. Gene Ther. 14 (2003) 1–12.
[8] Y. Zhang, F. Schlachetzki, Y.F. Zhang, R.J. Boado, W.M. Pardridge, Normalization of striatal tyrosine hydroxylase and reversal of motor impairment in experimental parkinsonism with intravenous nonviral gene therapy and a brain-specific promoter, Hum. Gene Ther. 15 (2004) 339–350.
[9] N.K. Gonatas, A. Stieber, W.F. Hickey, S.H. Herbert, J.O. Gonatas, Endosomes and golgi vesicles in adsorptive and fluid phase endocytosis, J. Cell Biol. 99 (1984) 1379–1390.
[10] A.K. Kumagai, J. Eisenberg, W.M. Pardridge, Absorptive-mediated endocytosis of cationized albumin and a b-endorphin-cationized albumin chimeric peptide by isolated brain capillaries. Model system of blood–brain barrier transport, J. Biol. Chem. 262 (1987) 15214–15219.
[11] D. Triguero, J.B. Buciak, W.M. Pardridge, Capillary depletion method for quantifying blood–brain barrier transcytosis of circulating peptides and plasma proteins, J. Neurochem. 54 (1990) 1882–1888.
[12] M. Thöle, S. Nobmann, J. Huwyler, A. Bartmann, G. Fricker, Uptake of cationized albumin coupled liposomes by cultured porcine brain microvessel endothelial cells and intact brain capillaries, J. Drug Target. 10 (2002) 337–344.
[13] C. Perez, A. Sanchez, D. Putnam, D. Ting, R. Langer, M.J. Alonso, Poly(lactic acid)–poly(ethylene glycol) nanoparticles as new carriers for the delivery of plasmid DNA, J. Control. Release 75 (2001) 211–224.
[14] Y.P. Li, M. Ogris, E. Wagner, J. Pelisek, M. Rüffer, Nanoparticles bearing polyethyleneglycol-coupled transferrin as gene carriers: preparation and in vitro evaluation, Int. J. Pharm. 259 (2003) 93–101.
[15] M.T. Peracchia, R. Gref, Y. Minamitake, A. Domb, N. Lotan, R. Langer, PEG-coated nanospheres from amphiphilic diblock and multiblock copolymers: investigation of their drug encapsulation and release characteristics, J. Control. Release 46 (1997) 223–231.
[16] M.F. Zambaux, F. Bonneaux, R. Gref, E. Dellacherie, C. Vigneron, Protein C-loaded monomethoxypoly(ethylene oxide)–poly(lactic acid) nanoparticles, Int. J. Pharm. 212 (2001) 1–9.
[17] P. Swayam, V. Labhasetwar, Critical determinants in PLGA/PLA nanoparticles-mediated gene expression, Pharm. Res. 21 (2004) 354–364.
[18] J. Panyam, V. Labhasetwar, Biodegradable nanoparticles for drug and gene delivery to cells and tissue, Adv. Drug Deliv. Rev. 55 (2003) 329–347.
[19] D. Bazile, C. Prud'homme, M.T. Bassoullet, M. Marlard, G. Spenlehauer, M. Veillard, Stealth Me.PEG–PLA nanoparticles avoid uptake by the mononuclear phagocyte system, J. Pharm. Sci. 84 (1995) 493–498.
[20] J.P. Plard, D. Bazile, Comparison of the safety profiles of PLA_{50} and Me.PEG–PLA_{50} nanoparticles after single dose intravenous administration to rats, Colloids Surf., B Biointerfaces 16 (1999) 173.
[21] J.C. Olivier, R. Huertas, H.J. Lee, F. Calon, W.M. Pardridge, Synthesis of pegylated immunonanoparticles, Pharm. Res. 19 (2002) 1137–1143.
[22] Y. Zhang, Q.Z. Zhang, L.S. Zha, W.L. Yang, C.C. Wang, X.G. Jiang, S.K. Fu, Preparation, characterization and application of pyrene-loaded methoxy poly(ethylene glycol)–poly(lactic acid) copolymer nanoparticles, Colloid Polym. Sci. 282 (2004) 1323–1328.
[23] Y. Dong, S.S. Feng, Methoxy poly(ethylene glycol)–poly (lactide) (MPEG–PLA) nanoparticles for controlled delivery of anticancer drugs, Biomaterials 25 (2004) 2843–2849.
[24] G.L. Ellmann, Tissue sulfhydryl groups, Arch. Biochem. Biophys. 82 (1959) 70–77.
[25] P.D. Scholes, A.G.A. Coombes, L. Illum, S.S. Davis, J.F. Watts, C. Ustariz, et al., Detection and determination of surface levels of poloxamer and PVA surfactant on biodegradable nanospheres using SSIMS and XPS, J. Control. Release 59 (1999) 261–278.
[26] S.S. Feng, L. Mu, K.Y. Win, G.F. Huang, Nanoparticles of biodegradable polymers for clinical administration of paclitaxel, Curr. Med. Chem. 11 (2004) 413–424.
[27] J. Davda, V. Labhasetwar, Characterization of nanoparticle uptake by endothelial cells, Int. J. Pharm. 233 (2002) 51–59.
[28] J. Panyam, S.K. Sahoo, S. Prabha, T. Bargar, V. Labhasetwar, Fluorescence and electron microscopy probes for cellular and tissue uptake of poly(D,L-lactide-co-glycolide) nanoparticles, Int. J. Pharm. 262 (2003) 1–11.
[29] S. Méresse, M.P. Dehouck, P. Delorme, M. Bensaid, J.P. Tauber, C. Delbart, et al., Bovine brain endothelial cells

express tight junctions and monoamine oxidase activity in long-term culture, J. Neurochem. 53 (1989) 1363–1371.
[30] R. Cecchelli, B. Dehouck, L. Descamps, L. Fenart, V. Buée-Scherrer, C. Duhem, et al., In vitro model for evaluating drug transport across the blood–brain barrier, Adv. Drug Deliv. Rev. 36 (1999) 165–178.
[31] Ph. Demeuse, A. Kerkhofs, C. Struys-Ponsar, B. Knoops, C. Remacle, Ph. van den Bosch de Aguilar, Compartmentalized coculture of rat brain endothelial cells and astrocytes: a syngenic model to study the blood–brain barrier, J. Neurosci. Methods 121 (2002) 21–31.
[32] Y.Z. Tan, Basic fibroblast growth factor-mediated lymphangiogenesis of lymphatic endothelial cells isolated from dog thoracic ducts: effects of heparin, Jpn. J. Physiol. 48 (1998) 133–141.
[33] P. Calvo, B. Gouritin, H. Chacun, D. Desmaële, J. D'Angelo, J.P. Noel, et al., Long-circulating PEGylated polycyanoacrylate nanoparticles as new drug carrier for brain delivery, Pharm. Res. 18 (2001) 1157–1166.
[34] M. Huang, E. Khor, L.Y. Lim, Uptake and cytotoxicity of chitosan molecules and nanoparticles: effects of molecular weight and degree of deacetylation, Pharm. Res. 21 (2004) 344–353.
[35] P. Bergmann, R. Kacenelenbogen, A. Vizet, Plasma clearance, tissue distribution and catabolism of cationized albumin with increasing isoelectric points in the rat, Clin. Sci. 67 (1984) 35–43.
[36] P. Quellec, R. Gref, L. Perrin, E. Dellacherie, F. Sommer, J.M. Verbavatz, M.J. Alonso, Protein encapsulation within polyethylene glycol-coated nanospheres: I. Physicochemical characterization, J. Biomed. Mater. Res. 42 (1998) 45–54.
[37] S. Prabha, Vinod Labhatsewar, Critical determinants in PLGA/PLA nanoparticle-mediated gene expression, Pharm. Res. 21 (2004) 354–364.
[38] S.M. Moghimi, C.J.H. Porter, I.S. Muir, L. Illum, S.S. Davis, Non-phagocytic uptake of intravenously injected microspheres in rat spleen: influence of particles size and hydrophilic coating, Biochem. Biophys. Res. Commun. 177 (1991) 861–866.
[39] H.Q. Mao, K. Roy, V.L. Troung-Le, K.A. Janes, K.Y. Lin, Y. Wang, et al., Chitosan-DNA nanoparticles as gene carriers: synthesis, characterization and transfection efficiency, J. Control. Release 70 (2001) 399–421.
[40] P. Quellec, R. Gref, E. Dellacherie, F. Sommer, M.D. Tran, M.J. Alonso, Protein encapsulation within poly(ethylene glycol)-coated nanospheres: II. Controlled release properties, J. Biomed. Mater. Res. 47 (1999) 388–395.
[41] A.W. Vorbrodt, Ultracytochemical characterization of anionic sites in the wall of brain capillaries, J. Neurocytol. 18 (1989) 359–368.
[42] J. Panyam, V. Labhasetwar, Dynamics of endocytosis and exocytosis of poly(D,L-lactide-co-glycolide) nanoparticles in vascular smooth muscle cells, Pharm. Res. 20 (2003) 212–220.
[43] D.E. Griffin, J. Giffels, Study of protein characteristics that influence entry into the cerebrospinal fluid of normal mice and mice with encephalitis, J. Clin. Invest. 70 (1982) 289–295.
[44] S. Hanafusa, Y. Matsusue, T. Yasunaga, T. Yamamuro, M. Oka, Y. Shikinami, Y. Ikada, Biodegradable plate fixation of rabbit femoral shaft osteotomies. A comparative study, Clin. Orthop. 315 (1995) 262–271.
[45] Y. Matsusue, S. Hanafusa, T. Yamamuro, Y. Shikinami, Y. Ikada, Tissue reaction of bioabsorbable ultra high strength poly (L-lactide) rod. A long-term study in rabbits, Clin. Orthop. 317 (1995) 246–253.
[46] D. Putnam, C.A. Gentry, D.W. Pack, R. Langer, Polymer-based gene delivery with low cytotoxicity by a unique balance of side-chain termini, Proc. Natl. Acad. Sci. U. S. A. 98 (2001) 1200–1205.